Experimental Study on Laser Induced Protrusion in HAMR

Haoyu Wang[*], Qilong Cheng, and David B. Bogy

Computer Mechanics Laboratory

University of California, Berkeley

September, 2019

[*]Summer intern, Shanghai Jiao Tong University

Contents

1 Introduction

1.1 Background

As the demand on information storage is rising, it is crucial to increase the areal density of traditional storage devices. Currently the limit of the areal density in the product-level magnetic media is about 1 TB/in^2 in **Hard Disk Drives (HDDs)** shown in Fig. 1. Higher density among current technology is no longer possible because of the superparamagnetic effect: if the size of the magnetic bits is further decreased, the bits will be thermally unstable. At room temperature, the random thermal fluctuations of media molecules have the strength to overcome the energy barrier between "up" and "down" magnetic orientations, thereby demagnetizing the bit grains and corrupting the stored magnetic data[1]. The industry has reached a consensus that the technology of **Heat Assisted Magnetic Recording (HAMR)** can realize higher storage density of HDDs.

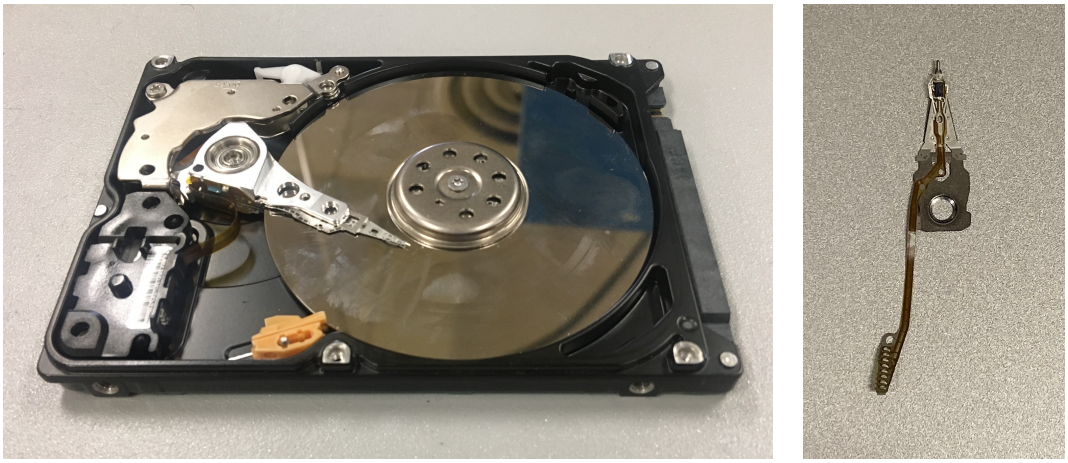

Figure 1: Modern HDD with cover plate removed and the HAMR waveguide head used in the experiments

1.2 Heat Assisted Magnetic Recording

HAMR technology uses a new kind of magnetic media which is stable at room temperature, but with a higher coercivity than traditional HDD media[1]. Fig. 2 shows a schematic diagram of the **Head-Disk Interface (HDI)** in HAMR. The slider is located at the end of the suspension. It has a designed and etched surface called the **Air Bearing Surface (ABS)**. When the disk is rotating, an air bearing is formed due to the ABS and the slider is thus lifted to ensure a gap of around 10∼20 nm.

There are several electrical elements near the trailing edge of the slider. In addition to the reading and writing elements, a **Thermal Fly-height Control (TFC)** element induces a local thermal protrusion to decrease the spacing and make other elements closer to the magnetic media, which is shown in Fig 3. Then the Laser creates a hot spot on the media and locally heats the magnetic layer to lower its coercivity such that data can be written. The spacing is thereby reduced to 1∼2 nm during data writing and reading[2].

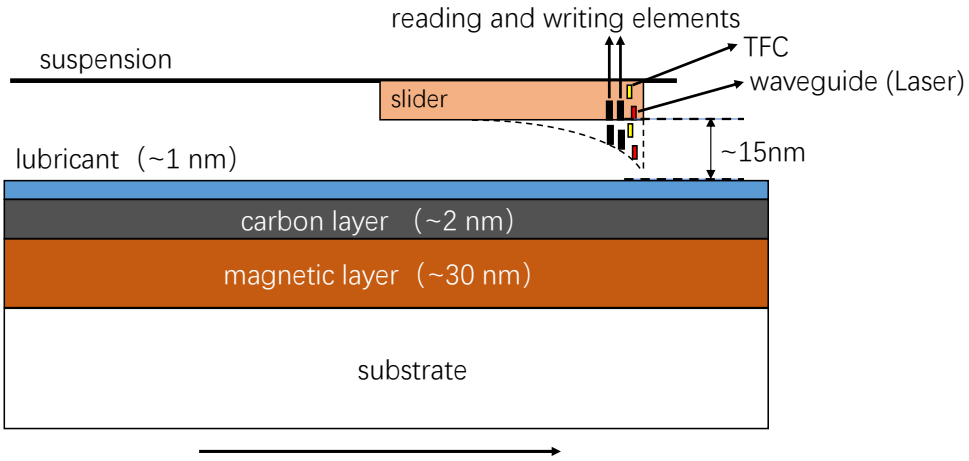

Figure 2: Schematic diagram of HAMR HDI

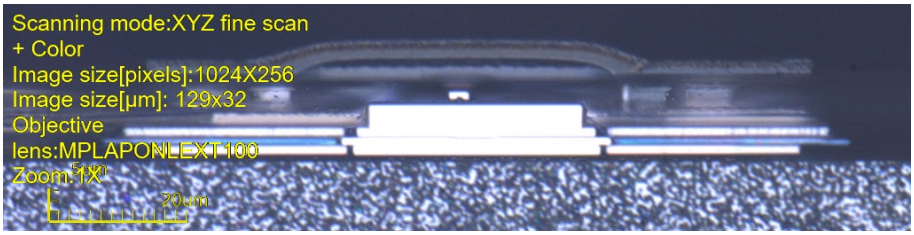

Figure 3: Elements near the trailing edge of the slider

1.3 Notations

The abbreviations in this report are listed below. Some of them are defined later in the following sections.

Table 1: Abbreviations and explanations

Abbreviation	Name
HDD	Hard Disk Drive
HAMR	Heat Assisted Magnetic Recording
HDI	Head-Disk Interface
ABS	Air Bearing Surface
TFC	Thermal Flight-height Control
TDP	Touchdown Power
NFT	Near Field Transducer
LDV	Laser Doppler Vibrometry
AE	Acoustic Sensor
DAQ	Data Acquisition Toolbox
RMS	Root Mean Square
FFT	Fast Fourier Transform

2 Experimental Setup and Research Goals

2.1 Experimental Setup

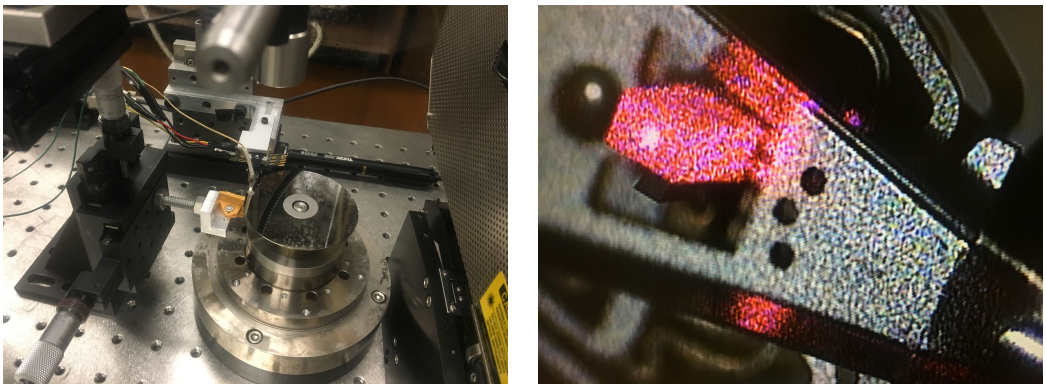

Figure 4: Experimental setup and the back of slider showing LDV laser spot

The component-level experiments are performed on a Candela spin-stand stage as shown above in Fig. 4. The HAMR waveguide head is mounted on a XYZ stage where the flying condition (linear velocity, skew angle, z height, etc.) can be changed. Note that the HAMR head is a waveguide-only head without a **Near Field Transducer (NFT)**. A **Laser Doppler Vibrometry (LDV)** spot is irradiated on the back of the slider to measure the vertical vibrations. Also, an **Acoustic Emission (AE)** sensor is glued on the fixture to acquire waves excited by head-disk contact.

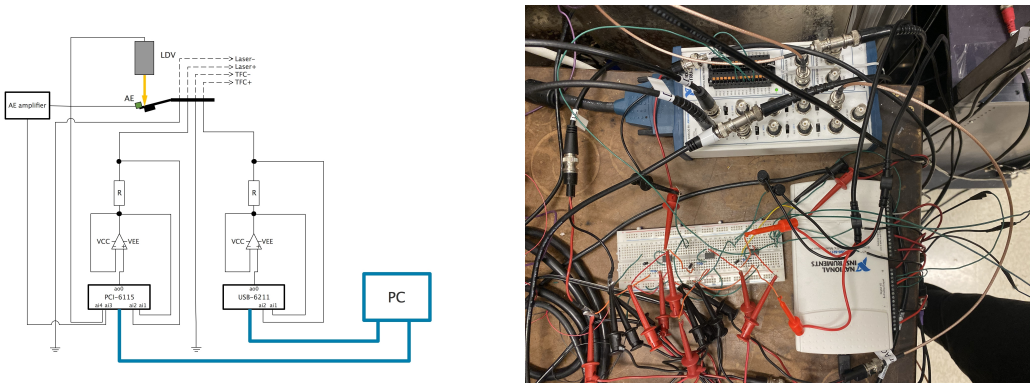

Figure 5: The design and the practical connection of the circuit

We use two **Data Acquisition (DAQ)** toolboxes to power the elements in the slider and measure their resistances. As shown above in Fig. 5, a USB-6211 DAQ uses a voltage source to power the TFC and a dummy resistance (50 Ω) and measures their total voltage and the voltage of the TFC itself, respectively. A PCI-6115 DAQ uses the same way to measure the Laser's current and voltage and collects the signals of the AE and LDV simultaneously.

2.2 Research Goals

We ramp up the TFC power to decrease the spacing until contact happens, where the TFC power is called **Touchdown Power (TDP)**. In HAMR, the Laser causes extra protrusion due to the laser

heating and affects the TDP. This report focuses on the TDP decrease caused by the Laser and the time for the Laser induced protrusion to reach equilibrium. Furthermore, we analyze vibration patterns of the slider during overpush flying experiments to understand the slider dynamics.

3 Results and Analysis

In HAMR, a Laser is introduced to heat the magnetic layer in order to decrease its coercivity. Meanwhile, it also heats the slider and causes extra protrusion since the output power of the Laser cannot be completely converted into optical power. This laser induced protrusion is determined by many factors, including the value of the Laser current, the linear velocity of the slider, and the time the Laser is turned on. The size of the Laser induced protrusion is measured by the TDP decrease caused by the Laser, since every 10 mW TFC power brings about 1 nm protrusion[3]. This section discusses how to measure the Laser time constant and the protrusion size under a specific scheme. At the same time, we use the data of AE and LDV to analyze the vibration patterns of the slider when it is in contact with the disk.

3.1 Laser Calibration

First, the I-V characteristics of the Laser diode is measured. The Laser diode does not output any light when its bias voltage is less than 1.3 V. Then the Laser current increases with a higher bias voltage. The Laser current v. Laser voltage is shown in Fig. 6. We use this curve to control the Laser current at a reasonable value in the following experiments.

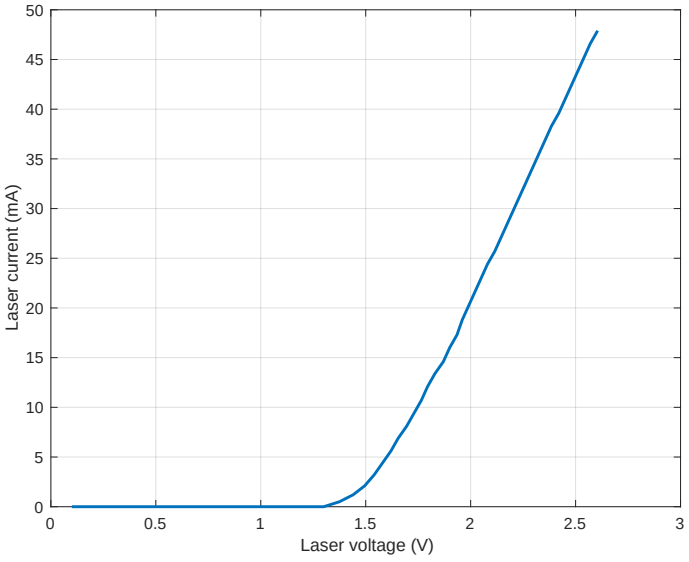

Figure 6: Laser current v. Laser voltage of the HAMR waveguide head

3.2 Laser Induced Protrusion

3.2.1 Experiment Scheme

During each sampling time, we turn on the TFC at $t = 20$ ms for a duration of 60 ms. Then at $t = 80$ ms we apply a voltage to the Laser with a specific pulse width. Note that now the TFC is still turned on. Finally we turn off the TFC and Laser together at 20 ms before the end of the sampling period. Since we are interested in the Laser time constant, the Laser pulse width is a variable in different tests. Therefore, the TFC pulse width and the sampling time both depend on

the Laser pulse width. For example, when it is 60 ms, as shown in Fig. 7, we have

$$\begin{aligned}\text{TFC pulse width} &= 60\text{ ms} + \text{Laser pulse width}\\ &= 60\text{ ms} + 60\text{ ms}\\ &= 120\text{ ms},\end{aligned}$$

$$\begin{aligned}\text{Sampling time} &= 20\text{ ms} + 60\text{ ms} + \text{Laser pulse width} + 20\text{ ms}\\ &= 100\text{ ms} + \text{Laser pulse width}\\ &= 100\text{ ms} + 60\text{ ms}\\ &= 160\text{ ms}.\end{aligned}$$

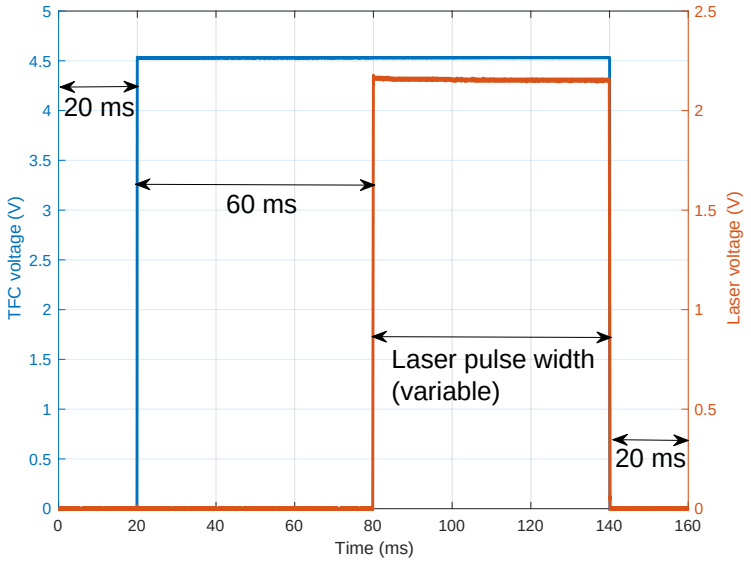

Figure 7: A typical sampling time when the Laser pulse width is 60 ms

In addition, the TFC power is increased by 0.5 mW each step, while the Laser current stays the same, at 28 mA, in each sampling time. Since the Laser pulse width affects the size of its caused extra protrusion before it gets to equilibrium, we test different values to the Laser pulse width to see how long it takes to reach equilibrium.

For example, the Laser pulse width 60 ms is shown in Fig. 8, which shows the transient signals of the AE under different TFC powers. The red line at 0.08 s of each figure is the time when the Laser is turned on. We call the first 60 ms in each sampling time when the TFC is turned on and the Laser is turned off, the Laser-off regime. Similarly, when the TFC and Laser are both turned on, we call it the Laser-on regime. When the TFC power is (a)168.90 mW, there is no contact, which we call **Flying State**[4]. When the TFC power is (b)170.90 mW, after the Laser is turned on, the protrusion is larger than that in the Laser-off, and contact happens in this regime. This is when the slider starts to make contact with the highest asperities of the disk. It is in the **Bouncing State** while in the Laser-off it stays at the Flying State. This effect gets stronger when the TFC power is (c)173.90 mW. Then when it is (d)175.42 mW, the protrusion in the Laser-off contacts with the disk. As the TFC power rises, the contact becomes more intense.

The signals in the Laser-off is stronger than that in the Laser-on, as shown in (f), most likely because the protrusion remains in contact with the lubricant and causes some burnishing of the disk. The slider comes into the **Surfing State** in the Laser-on, resulting from the extra heat from the Laser, while in the Laser-off it is still in the Bouncing State.

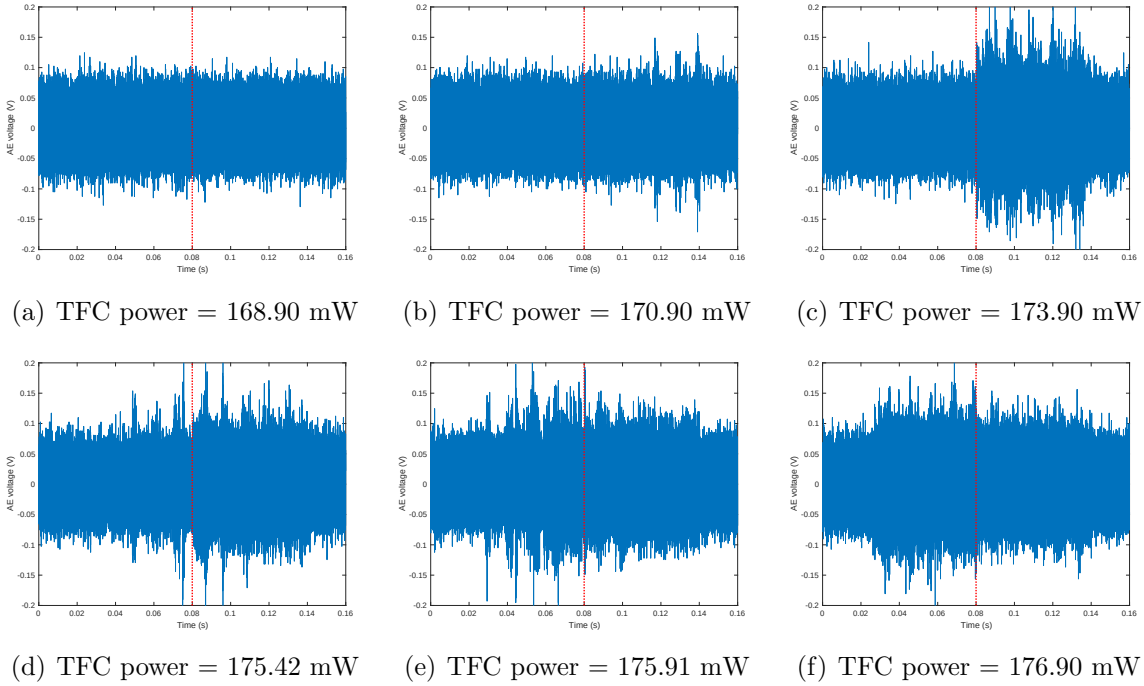

(a) TFC power = 168.90 mW (b) TFC power = 170.90 mW (c) TFC power = 173.90 mW

(d) TFC power = 175.42 mW (e) TFC power = 175.91 mW (f) TFC power = 176.90 mW

Figure 8: Transient AE signals drawing a single sampling time under different TFC powers when the Laser pulse width is 60 ms

3.2.2 TDP Definition

We calculate **Root Mean Square (RMS)** on these two regimes, Laser-on and Laser-off, respectively. As shown in Fig. 9, the shapes of the two curves are similar, with some delay in between. This confirms our assumption that the Laser causes extra protrusion and earlier contact in terms of the TFC power. As shown by the curves, the differences in the three states are obvious. The AE RMS of the Flying State remains almost constant at a low value, and it suddenly rises when contact happens. After dropping it gets into the Surfing State and remains there at a relatively higher value than in the Flying State.

The two green markers in the zoom-in picture of Fig. 9(b) represent the TFC powers where contact appears in the AE transient signals. They are at TFC power (c)169.91 mW on the orange curve and (d)174.14 mW on the blue curve. For lower power there is no contact indicated.

However, this marker does not indicate when the touchdown happens exactly. It may happen between the marker and the data point before it. We define the real TDP as follows:

1. Calculate the average of the points' AE RMS before the marker, and set the average as the baseline;

2. Set 105% of the baseline as the standard of touchdown[2];

3. According to the standard, do a linear interpolation between the marker and the data point before it;

4. The result of the linear interpolation at the standard of the touchdown is the TDP;

5. The difference between the two TDPs of the two curves is the TDP decrease caused by the Laser.

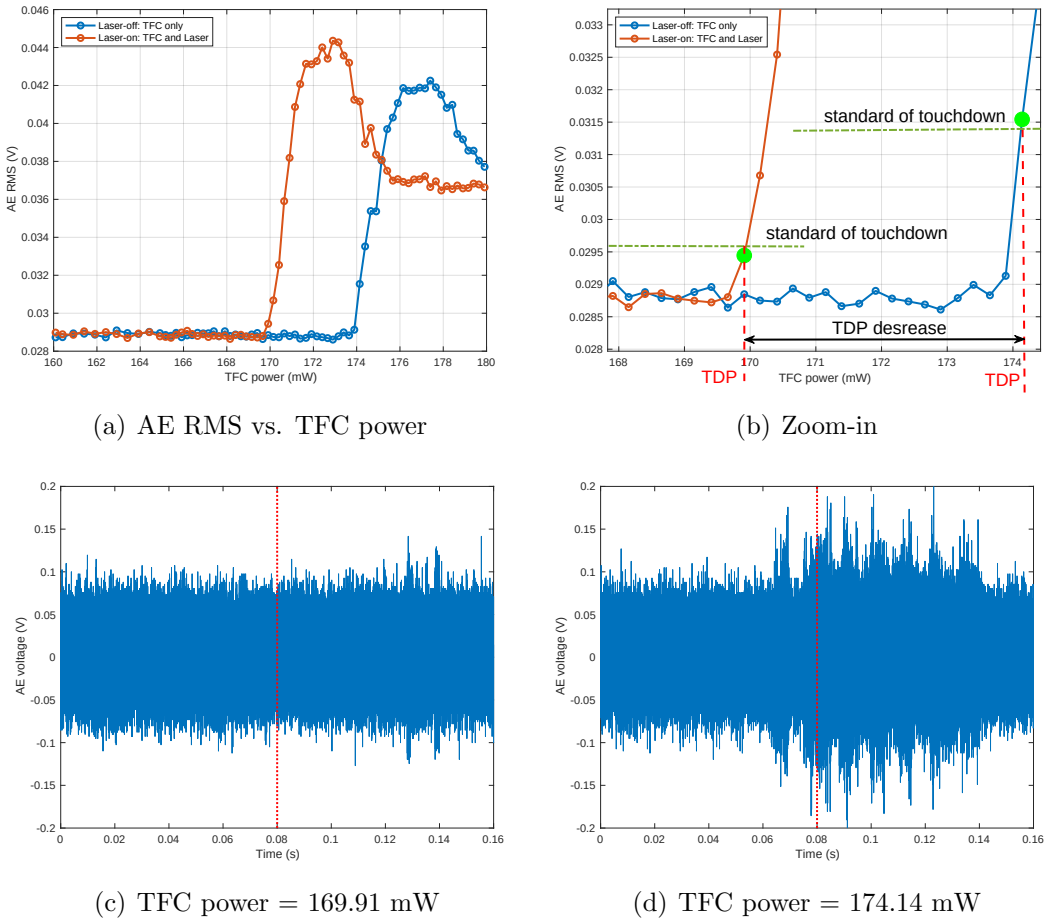

(a) AE RMS vs. TFC power

(b) Zoom-in

(c) TFC power = 169.91 mW

(d) TFC power = 174.14 mW

Figure 9: Find touchdown power according to AE RMS and AE transient signals. The Laser pulse width during each sampling time is 60 ms.

Using this method we have determined that when the Laser pulse width is 60 ms, the TDP of the Laser-on is 170.08 mW and for Laser-off it is 174.02 mW. The Laser with 60 ms pulse width causes a TDP decrease by 3.94 mW. Therefore, the Laser induced protrusion measures about 0.4 nm under such condition, since every 10 mW TFC power brings about 1 nm protrusion[3].

3.2.3 Laser Time Constant

According to our measurement, for a fixed Laser pulse width we get a determined TDP decrease. Next, we changed the Laser pulse width between 0 ms and 100 ms and implemented the method

aforementioned. The relationship between the Laser pulse width and the TDP decrease is shown in Fig. 10.

In the experiments, the HAMR head is flying over a 5400 RPM glass disk at the OD (linear velocity is 16.3 m/s) and the Laser current is 28 mA. The TDP decrease that represents the Laser induced protrusion at first rises rapidly with Laser pulse width as seen in Fig. 10. When the Laser pulse width comes to about 35 ms, the TDP decrease reaches its steady state, about 4 mW. It shows that under such conditions the Laser needs about 35 ms to get to equilibrium. In the last section, the Laser pulse width was 60 ms which meant that the Laser induced protrusion had reached equilibrium.

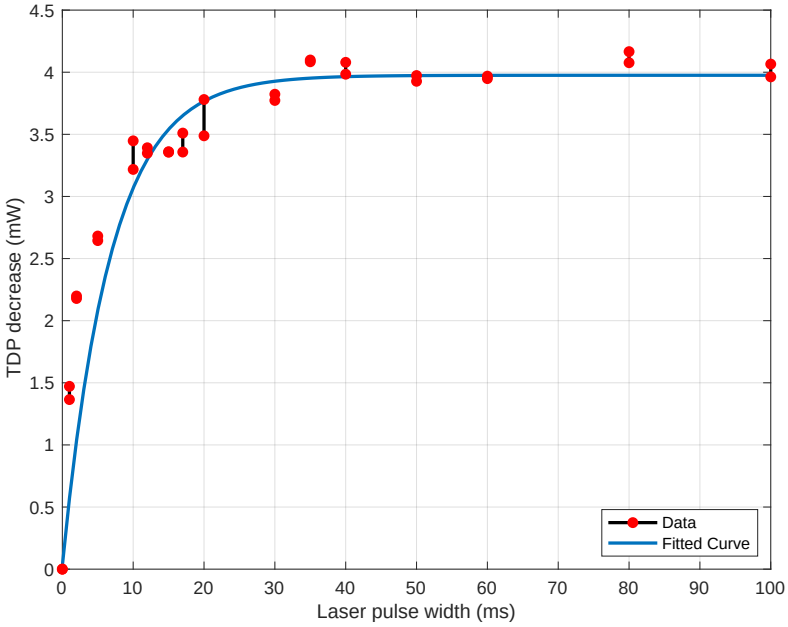

Figure 10: Laser pulse width vs. TDP decrease

3.3 Slider Dynamics Frequency Analysis

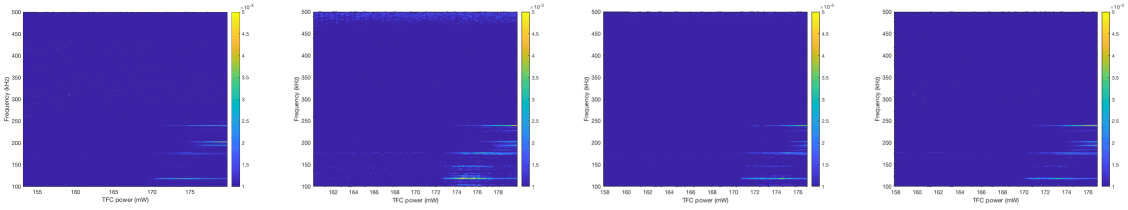

(a) Laser pulse width = 0 ms (b) Laser pulse width = 20 ms (c) Laser pulse width = 50 ms (d) Laser pulse width = 80 ms

Figure 11: The relationship between slider vibration frequency and TFC power under different Laser pulse widths

Next, we perform a **Fast Fourier Transform (FFT)** on the Laser-off and Laser-on regimes. Fig. 11 shows no qualitative difference in the vibration pattern among tests with different Laser pulse

widths.

Consider a Laser pulse width of 20 ms for detailed analysis. When the TFC power is 171.9 mW contact happens and three frequencies, 119 kHz, 146 kHz, and 177 kHz, appear as shown in Fig. 12. At the power of 175.2 mW the contact becomes more intense and 240 kHz becomes obvious. At 177.4 mW the slider gets into Surfing State and 146 kHz disappears while two more peaks, around 200 kHz emerge.

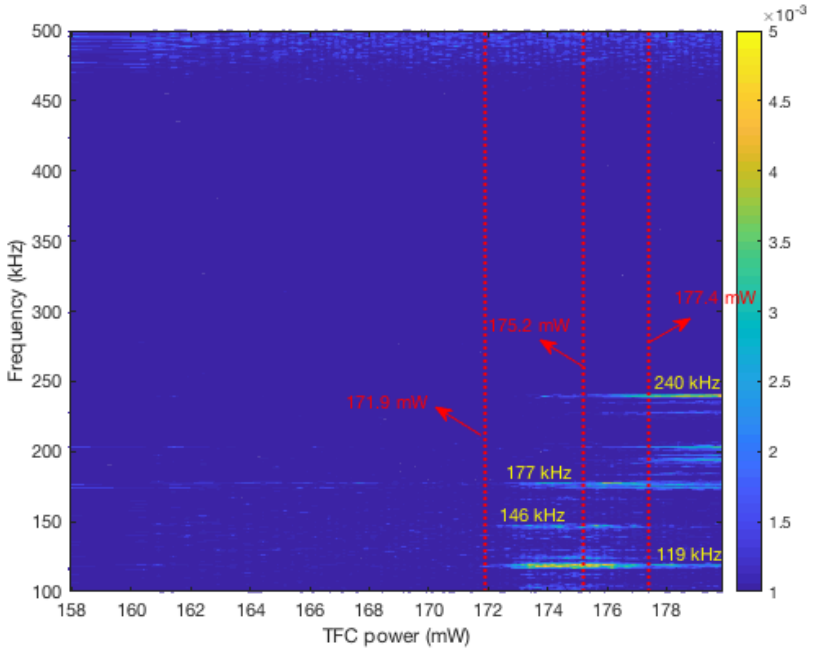

Figure 12: Frequency vs. TFC power when Laser pulse width is 20 ms

4 Conclusions

When the glass substrate disk is rotating at 5400 rpm, the HAMR head flies at the OD (linear velocity 16.3 m/s), and the Laser current is 28 mA, the Laser needs 35 ms to reach equilibrium and causes a TDP decrease by 4 mW, which corresponds to the protrusion of around 0.4 nm.

The method we presented in this report can also be applied to other conditions (different velocities and Laser currents) for further research. One advantage of this method is that during each test, although the slider might get contaminated and the TDP could change, this method calculates the difference of TDPs in two regimes that are implemented simultaneously. So even if the slider is not clean from test to test, which indicates inconsistent initial conditions, the results will not be affected.

Acknowledgement

It would be impossible to complete this summer research project without the support of several people at the Computer Mechanics Laboratory, University of California, Berkeley.

First, I would like to thank the director of CML, Professor David B. Bogy for offering me the opportunity to work in his lab. Prof. Bogy comes to the lab every day and discusses with us, not only about our research progress, but also caring about our personal development. Prof. Bogy encourages me to persist in my goal and introduces me to Prof. Savas, another professor specialized in the area of my interest. Also, I am very grateful for Prof. Bogy's patient guidance about my research, especially for my first few weeks in Berkeley, whose enthusiasm towards research teaches me a lot.

Second, I would like to thank Qilong Cheng for introducing me to the topic, and teaching me about DAQ programming, experimental design, and data analysis. He has been very helpful throughout my entire research, guiding me on how to do research and how to give presentations properly. I greatly appreciate his patient mentoring.

Last but not least, I would like to thank Amin Ghafari and Siddhesh Sakalkar for insightful discussion about my project and personal development.

References

[1] Joanna B. Dahl. *Heat Assisted Magnetic Recording Head-Disk Interface: Numerical Simulation of Air Bearing and Lubricant Mechanics*. PhD thesis, University of California, Berkeley, 2013.

[2] Yuan Ma. *Study of Dynamics and Nanoscale Heat Transfer of Head Disk Interface in Hard Disk Drives*. PhD thesis, University of California, Berkeley, 2018.

[3] Haoyu Wu. *A Study of the Head Disk Interface in Heat Assisted Magnetic Recording - Energy and Mass Transfer in Nanoscale*. PhD thesis, University of California, Berkeley, 2018.

[4] Yuna-Kan Chen, Jinglin Zheng, and David B. Bogy. Light contact and surfing state dynamics of air bearing sliders in dard disk drives. *Applied Physics Letters*, 100, 2012.

[5] Siddhesh V. Sakhalkar and David B. Bogy. Effect of rheology and slip on lubricant deformation and disk-to-head transfer during heat-assisted magnetic recording (hamr). *Tribology Letters*, 66, 2018.

[6] Yuan Ma, Amin Ghafari, Bair V. Budaev, and David B. Bogy. Measurement and simulation of nanoscale gap heat transfer using a read/write head with a contact sensor. *IEEE Transactions on Mechanics*, 53(2), 2017.

[7] Yuna-Kan Chen. *Some Tribological Aspects of the Hard Disk Drive Head-Disk Interface for Quasi Contact Conditions: Contact Detection, Lubricant Modulation and Wear*. PhD thesis, University of California, Berkeley, 2015.

[8] Yuna-Kan Chen, Jih-Ping Peng, and David B. Bogy. Thermal protrusion-induced air bearing slider instability at disk proximity and light contact. *IEEE Transactions on Mechanics*, 50(7), 2014.

[9] Q. H. Zeng, Brian H. Thornton, David B. Bogy, and C. Singh Bhatia. Flyability and flying height modulation measurement of sliders with sub-10 nm flying. *IEEE Transactions on Mechanics*, 37(2), 2001.

[10] Shaomin Xiong and David B. Bogy. Flying height modulation for a dual thermal protrusion slider in heat assisted magnetic recording (hamr). *IEEE Transactions on Mechanics*, 49(10), 2013.